TECHNICAL NOTE
D-1298

THEORY OF HIGH-SPEED-IMPACT ATTENUATION

BY GAS BAGS

By John Thomas Howe

Ames Research Center
Moffett Field, Calif.

NATIONAL AERONAUTICS AND SPACE ADMINISTRATION

WASHINGTON April 1962

1V

NATIONAL AERONAUTICS AND SPACE ADMINISTRATION

TECHNICAL NOTE D-1298

THEORY OF HIGH-SPEED-IMPACT ATTENUATION BY GAS BAGS

By John Thomas Howe

SUMMARY

A theory is developed for the one-dimensional motion of a cylindrical gas bag used as an impact cushion. The effect of shock waves in the gas as well as stress in the bag skin is considered. The applicability of the theory to landings both in an atmosphere and on the moon is discussed and the regime of validity of the theory is presented. The use of a series expansion for computing shock-wave properties in the analysis, the strong shock approximation, and the exact shock relations are compared and discussed. The regime of physical parameters for which both the wave model and the series expansion are valid is presented. The method of application of the theory to impact problems is outlined.

INTRODUCTION

Over the past five years there has been a growing interest in impact attenuation. Considerable experimental and some theoretical work has been done on the study of impact. Drop tests have been performed at the University of Texas (refs. 1 to 5) using numerous impact attenuation techniques, including crushable structures, foamed plastics, and inflated cylindrical bags. Most of that work was performed at low impact speeds. The use of inflated bags for cushioning the impact of ejected aircraft pilot compartments has been investigated, as well as impact attenuation associated with atmosphere entry vehicles (refs. 6 to 8). A theory of low-speed impact of various shaped gas bags has been developed by Esgar and Morgan (ref. 9). Martin and Howe have developed a uniform compression theory for the impact of inflated spheres (ref. 10) as well as a theory which accounts, in an approximate way, for wave motion in the inflating gas (ref. 11). In these last two papers, a two-dimensional unsteady problem was simplified in various ways to achieve a workable analysis.

The problem in the present analysis has a simple one-dimensional geometry. For this reason, fewer assumptions need be made in the development of the theory. Basically, the problem has one space dimension and one time dimension as independent variables. The analysis is valid up to the time that the payload comes to rest. In solving this problem, it is necessary to couple the effects of the unsteady wave motion in the inflating gas with those of the structural behavior of the bag skin.

The latter aspect of the problem could be exceedingly difficult in itself if one attempted to solve it as an unsteady elasticity problem with a moving discontinuous load. This would introduce two space and one time dimension, which when combined with the unsteady gas dynamics might make solving the problem a virtually hopeless task. The waves in the skin would be coupled with the waves in the gas although the two would not move at the same speed and the motion of the payload would be exceedingly complicated.

Instead, we adopt a simple model for the bag, considering it to be a cylindrical membrane with high sound speed, and devote most of our attention to the wave motion in the inflating gas. The interaction of families of gas waves is examined, and a reasonable gas wave model is chosen for analysis. The conditions under which the model is valid are examined for impact on a planet with an atmosphere as well as on an airless surface. The property relationships across the shock waves in the gas are expressed in three ways: by the series expansion method and the strong shock approximation which have the advantage of analytical simplicity, and the exact method. The conditions that limit the use of the first two methods are discussed. Relationships for maximum acceleration, stopping distance (stroke), bag stresses, and pressures are derived from the theory.

SYMBOLS

A	cross-sectional area of cylindrical bag, and coefficients in equation (48)
c	sound speed in the inflating gas
$\tilde{c}$	dimensionless sound speed defined by equation (8)
F	forces in sketches (a) and (b)
g	gravitational constant at the earth's surface
K	defined by equation (11)
m	mass
m_b	mass of sides of bag
n	allowable number of g's acceleration
N	force per unit length
p	pressure

r	cross-sectional radius of cylindrical bag
R	gas constant
t	time
$\bar{t}$	dimensionless time defined by equation (14)
T	temperature
u	velocity in positive y direction
$\bar{u}$	dimensionless velocity defined by equation (8)
V	instantaneous volume of gas bag
W	shock speed relative to gas at state 1
x	defined by equation (49)
y	distance normal to impact surface (positive outward)
$\bar{y}$	dimensionless distance defined by equation (8)
α, β, τ, μ	defined by equation (23)
γ	ratio of specific heats of inflating gas
ρ	mass per unit surface area

Subscripts

$0, 1, 2, 3$	states shown on sketch (d), and subscripts on coefficients in equation (48)
$01, 12, 23$	shock connecting states 0 and 1, 1 and 2, 2 and 3
a	point on sketches (c) and (d) or atmosphere, axial
b	point on sketches (c) and (d) or side walls of bag
c	point on sketches (c) and (d) or circumferential
d, e, f	points on sketches (c) and (d)
g	inflating gas

i	condition ahead of a shock
j	conditions behind a shock
p	payload
bottom	bottom of bag

ANALYSIS

The Equation of Motion

Consider a nonslender[1] cylindrical bag of height y_o and cross-sectional area A. The bag is inflated to a pressure p_o. On top of the bag is a payload of mass m_p. The pressure on the outside of the payload is p_a. It is assumed that the bag is stiff enough to remain cylindrical under $p_o - p_a$. The system moves along the axis of the right cylinder with speed $|u_o|$ and strikes a flat surface normal to the cylinder axis. During the impact, the pressure in the inflating gas at the payload is p (at height y above the surface). A free body diagram of the payload is shown in sketch (a) (where it is assumed that the bottom of the payload is flat and always normal to the axis). The momentum theorem applied to

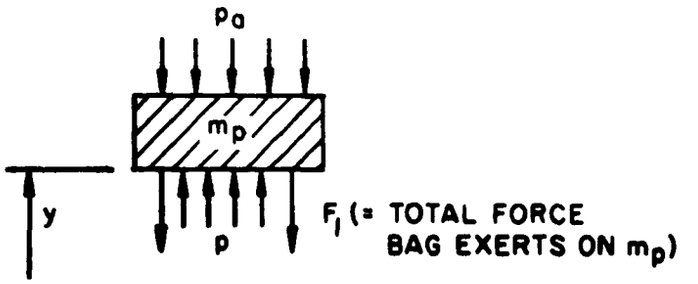

Sketch (a)

that free body is, with gravity forces neglected,

$$m_p\ddot{y} = (p - p_a)A - F_1 \tag{1}$$

---

[1]A nonslender bag is defined as one not subject to long column type buckling. For the case of a circular cylindrical bag and low impact speed, it appears that if the diameter is less than about 75 percent of the initial bag height, the gas bag buckles and is unstable (ref. 5).

A free body diagram of the sides of the bag, excluding the gas, is shown in sketch (b). In time dt, the skin changes momentum by the amount $m_{sv}du$

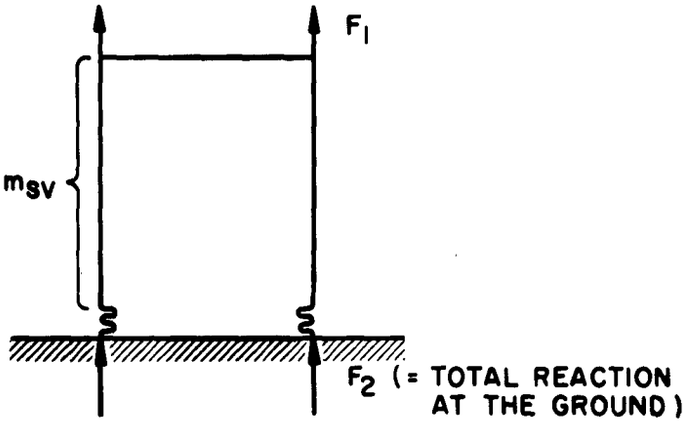

Sketch (b)

as a result of a change in velocity (where m_{sv} is the bag mass in motion). In the same time, the momentum change due to a change in mass is $dm_{sv}(u)$. The total momentum change is $m_{sv}du + dm_{sv}(u) = (F_1 + F_2)dt$, where shear forces due to gas or atmosphere are neglected or

$$\frac{d}{dt}(m_{sv}u) = F_1 + F_2 \tag{2}$$

The force F_2 brings the mass dm_{sv} to rest in time dt. Here the unrestrictive assumption has been made that the tension goes to zero (the buckling stress of the bag) at the top of the element dm_{sv}.

$$F_2dt = u\,dm_{sv} \tag{3}$$

Therefore from equations (2) and (3)

$$F_1 = m_{sv}\frac{du}{dt} \tag{4}$$

From equations (1) and (4)

$$(m_p + m_{sv})\,u\,\frac{du}{dy} = (p - p_a)A \tag{5}$$

If m_b is the mass of the sides of the bag, then

$$m_{sv} = m_b \frac{y}{y_o} \tag{6}$$

$$\left(m_p + m_b \frac{y}{y_o}\right) u \frac{du}{dy} = (p - p_a)A \tag{7}$$

Let

$$\left.\begin{array}{lll} \bar{y} = \dfrac{y}{y_o} & dy = y_o d\bar{y} & \bar{p} = \dfrac{p}{p_o} \\ \bar{u} = \dfrac{u}{|u_o|} & du = |u_o| d\bar{u} & \bar{c} = \dfrac{c}{|u_o|} \end{array}\right\} \tag{8}$$

A 5 7 4

then

$$(m_p + m_b\bar{y}) \frac{u_o^2}{y_o} \bar{u} \frac{d\bar{u}}{d\bar{y}} = p_o A(\bar{p} - \bar{p}_a) \tag{9}$$

$$\frac{m_p u_o^2}{y_o p_o A}\left(1 + \frac{m_b}{m_p}\bar{y}\right) \bar{u} \frac{d\bar{u}}{d\bar{y}} = \bar{p} - \bar{p}_a \tag{10}$$

If K is defined as

$$K = \frac{y_o p_o A}{m_p u_o^2} = \frac{p_o V_o}{m_p u_o^2} = \frac{m_g}{m_p} \frac{RT_o}{u_o^2} = \frac{m_g}{m_p} \frac{\bar{c}_o^2}{\gamma} \tag{11}$$

then

$$\frac{d\bar{u}}{d\bar{y}} = \frac{K(\bar{p} - \bar{p}_a)}{\bar{u}[1 + (m_b\bar{y}/m_p)]} \tag{12}$$

By definition

$$\frac{d\bar{t}}{d\bar{y}} = \frac{1}{\bar{u}} \tag{13}$$

where

$$\bar{t} = \frac{t|u_o|}{y_o} \tag{14}$$

Now to integrate equations (12) and (13), we need initial conditions and a description of $\bar{p}$ and $\bar{p}_a$. For very low impact speeds (high $\bar{c}_o$) it is probably adequate to describe $\bar{p}$ by the isentropic relation

$$\bar{p}\bar{V}^{\gamma} = 1 \tag{15}$$

where

$$\bar{V} = \frac{V}{V_o} = \frac{y}{y_o} = \bar{y} \tag{16}$$

However, for high impact speeds, equation (15) is not adequate because shock and rarefaction waves move through the gas, and the pressure must be calculated accordingly. This will be considered in the next section.

Similarly, we need to express $\bar{p}_a$. On the moon, it is zero. In an atmosphere, the entire payload and inflated bag combination moving toward the surface has a flow field around it, a wake, and a stagnation region. When the bag strikes the surface, the flow is altered (including the wake) and the pressure in the immediate neighborhood of the system varies with space and time. A detailed treatment of this external flow field is obviously very complicated. Although various approximations to the external flow could be adopted, we adopt the simplest one possible and say that the external pressure on the payload is represented by an effective constant average, p_a. We now move on to the calculation of $\bar{p}$ by considering the wave motion in the inflating gas.

The Wave Model in the Inflating Gas

Sketch (c) represents the most general wave pattern in the inflating gas. The curve abfd is a trace of the payload motion in the space-time plane. The heavy curves represent the traces of shock waves and the dashed lines, those of rarefaction waves. At time zero, the bottom of the bag strikes the ground and shock wave ob propagates upward (analogous to the impulsively started piston). At or near time zero, stress relief in the bag skin changes the motion of the payload, ab, causing a rarefaction to propagate downward from ab. That rarefaction intersects the initial upward traveling shock at e. The shock is modified by the rarefaction and its trajectory eb is curved.

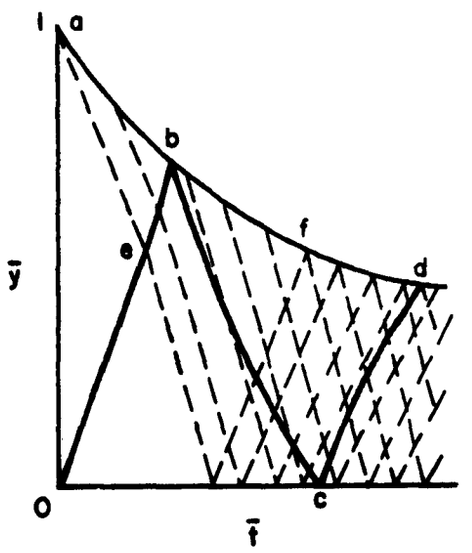

Sketch (c)

The shock then reflects from the bottom of the payload at b and the trajectory of the reflected shock bc is also curved. The reflected head of the initial rarefaction wave crosses the reflected shock and arrives at the payload at f. In general, the computation of the pressure at the payload depends on what happens in the entire wave system and is a difficult computation for the complete wave system shown in sketch (c).

On the other hand, if the change in forces (and motion) on the payload due to stress waves in the skin is negligible compared with that due to pressure waves in the gas, the wave pattern is much simpler (sketch (d)). This condition is approached if $\bar{p}_2 - \bar{p}_a \gg \bar{p}_o - \bar{p}_a$ and is exact if $\bar{p}_o = \bar{p}_a$ (no overpressure). Even if $\bar{p}_a$ is zero (lunar impact) the approximation is valid provided $\bar{p}_2$ is much larger than $\bar{p}_o$ (corresponding to small $\bar{c}_o$). We will adopt the simple wave pattern of sketch (d) and focus our attention only on cases where $\bar{p}_2 - \bar{p}_a \geq 10(1 - \bar{p}_a)$; the arbitrary factor 10 is considered conservative. Thus the paths ab and ob are straight lines. Paths bc and cd may be curved, but they do not influence the path bd or the computation of the pressure along bd except in locating point d. Subsequently, bc and cd will be treated as straight lines and will be discussed in detail.

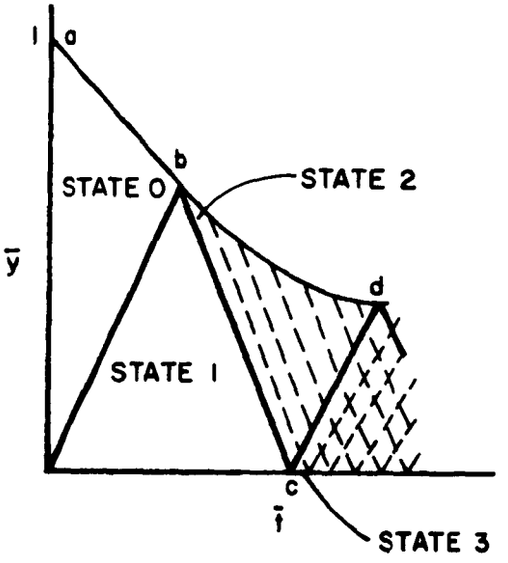

Sketch (d)

If the payload comes to rest before the point d is reached, the entire pressure computation is that of a simple wave (ref. 12, p. 413). In the simple wave region

$$\bar{c} + \frac{\gamma - 1}{2}\bar{u} = \bar{c}_2 + \frac{\gamma - 1}{2}\bar{u}_2 \qquad (17)$$

or

$$\frac{\bar{c}}{\bar{c}_2} = 1 - \frac{\gamma - 1}{2}\left(\frac{\bar{u} - \bar{u}_2}{\bar{c}_2}\right) \qquad (18)$$

and from isentropic relationships (noting that $\bar{u}_2 = -1$ since the slope of abd is continuous at b)

$$\frac{\bar{p}}{\bar{p}_2} = \left(\frac{\bar{c}}{\bar{c}_2}\right)^{\frac{2\gamma}{\gamma-1}} = \left[1 - \left(\frac{\gamma - 1}{2}\right)\left(\frac{\bar{u} + 1}{\bar{c}_2}\right)\right]^{\frac{2\gamma}{\gamma-1}} \tag{19}$$

Substituting equation (19) into (12) yields

$$\frac{d\bar{u}}{d\bar{y}} = \frac{K\left\{\bar{p}_2\left[1 - \frac{\gamma - 1}{2}\left(\frac{\bar{u} + 1}{\bar{c}_2}\right)\right]^{\frac{2\gamma}{\gamma-1}} - \bar{p}_a\right\}}{\bar{u}\left(1 + \frac{m_b}{m_p}\bar{y}\right)} \tag{20}$$

For convenience equation (13) is repeated

$$\frac{d\bar{t}}{d\bar{y}} = \frac{1}{\bar{u}} \tag{13}$$

The boundary conditions on equations (20) and (13) are at

at $\bar{y} = \bar{y}_b$

$$\left.\begin{aligned} \bar{u} &= -1 \\ \bar{t} &= \bar{t}_b \end{aligned}\right\} \tag{21}$$

Equations (20), (13), and (21) comprise the set of differential equations and their boundary conditions whose solution is the motion of the payload during impact. Before describing ways to obtain $\bar{p}_2$, $\bar{c}_2$, $\bar{y}_b$, and $\bar{t}_b$, it is instructive to integrate equation (20) formally for the case $\bar{p}_a = 0$.

Payload Velocity During Impact Without Atmosphere

Variables in equation (20) are at once separable (note that $\bar{p}_a$ is set to zero)

$$\frac{d\bar{y}}{1 + \frac{m_b}{m_p}\bar{y}} = \frac{1}{K\bar{p}_2} \frac{\bar{u}\, d\bar{u}}{\left(\frac{2\bar{c}_2 + 1 - \gamma}{2\bar{c}_2} - \frac{\gamma - 1}{2\bar{c}_2}\bar{u}\right)^{\frac{2\gamma}{\gamma-1}}} \tag{22}$$

Denoting

$$\left.\begin{aligned} \alpha &= \frac{2\bar{c}_2 + 1 - \gamma}{2\bar{c}_2} \\ \beta &= \frac{-(\gamma - 1)}{2\bar{c}_2} \\ \tau &= \frac{m_b}{m_p} \\ \mu &= \frac{-2\gamma}{\gamma - 1} \end{aligned}\right\} \qquad (23)$$

and noting that $\bar{p}_2$ and $\bar{c}_2$ are constants determined by initial conditions (as will be shown subsequently) we integrate equation (22) subject to boundary conditions (21). This gives (since $\mu \neq -1$ or -2)

$$\bar{y}(\bar{u}) = \left(\frac{1}{\tau} + \bar{y}_b\right)\exp\left\{\frac{\tau}{\beta^2 K \bar{p}_2}\left[\frac{(\alpha + \beta\bar{u})^{\mu+2} - 1}{\mu + 2} + \alpha\,\frac{1 - (\alpha + \beta\bar{u})^{\mu+1}}{\mu + 1}\right]\right\} - \frac{1}{\tau} \qquad (24)$$

Equation (24) represents the motion of the payload during impact in a vacuum. It does not appear to be readily integrable again in combination with (13) to yield $\bar{t}(\bar{y})$. Note that at $\bar{u} = 0$,

$$\bar{y}_{min} = \left(\frac{1}{\tau} + \bar{y}_b\right)\exp\left\{\frac{\tau}{\beta^2 K \bar{p}_2}\left[\frac{\alpha^{\mu+2} - 1}{\mu + 2} + \frac{\alpha(1 - \alpha^{\mu+1})}{\mu + 1}\right]\right\} - \frac{1}{\tau} \qquad (25)$$

For large $\bar{c}_0$, $\bar{c}_2$ is large and $\alpha \to 1$, so that

$$\bar{y}_{min} \to \bar{y}_b \qquad (26)$$

In the special solution of equation (25) and in the general problem, $\bar{p}_2$, $\bar{c}_2$, $\bar{y}_b$, and $\bar{t}_b$ are still not determined. These will now be determined from normal shock relationships.

Normal Shock Relationships

Having adopted a simple wave model and included it in the differential equation of motion of the payload, we now compute initial conditions just inside the simple wave region at b (sketch (d)) by three methods. The first method is a series expansion. It has the advantage of simplicity, and leads to explicit physical relationships. However, its validity is limited to certain regimes of impact conditions. The second method involves the use of exact shock relationships, and the third is the strong shock approximation.

Series expansion.- The series expansion relationships for properties across a moving shock are valid as long as the shock is not too strong. In the present paper the restriction on shock strength corresponds to a restriction on $\bar{c}_o$. It will be shown subsequently that if $\bar{c}_o \geq 1$, there will be an error in the series expansion computation of $\bar{p}_2$ and $\bar{y}_b$ of 10 percent or less (for $\gamma = 1.41$). This corresponds to a maximum value of $\bar{p}_2$ of roughly 9 for use of the series expansion.

In addition to this restriction associated with the series expansion, there is the further restriction associated with the wave model adopted in sketch (d). For the wave model to be adopted it was required that

$$\bar{p}_2 - \bar{p}_a \gg \bar{p}_o - \bar{p}_a = 1 - \bar{p}_a$$

If $\bar{p}_a = 0$, and since the upper limit on $\bar{p}_2 \approx 9$, it is seen that the inequality is not really satisfied in the strong sense by solutions using the series expansion. Thus the series expansion should not be used for impact without an atmosphere; the exact shock relations or strong shock relations should be used instead. On the other hand, if $\bar{p}_a = 1$, the inequality is always satisfied, the wave model in sketch (d) is applicable, and the series expansion can be used as long as $\bar{c}_o$ is greater than unity as mentioned above (but less than an upper bound that will be shown subsequently).

From sketch (d), it is seen that

$$\left.\begin{aligned} \bar{u}_o &= -1 \\ \bar{u}_1 &= 0 \\ \bar{u}_2 &= -1 \\ \bar{u}_3 &= 0 \end{aligned}\right\} \qquad (27)$$

The polynomial expansions of shock relations in terms of shock strength are (ref. 12, p. 1011).

$$\bar{c}_1 = \bar{c}_o + \frac{\gamma - 1}{2}(\bar{u}_1 - \bar{u}_o) + \ldots [0](\bar{u}_1 - \bar{u}_o)^3 \approx \bar{c}_o + \frac{\gamma - 1}{2} \tag{28}$$

$$\bar{c}_2 = \bar{c}_1 - \frac{\gamma - 1}{2}(\bar{u}_2 - \bar{u}_1) + \ldots [0](\bar{u}_2 - \bar{u}_1)^3 \approx \bar{c}_o + \gamma - 1 \tag{29}$$

$$\left(\frac{d\bar{y}}{d\bar{t}}\right)_{\text{shock ob}} \equiv \frac{\bar{u}_o + \bar{c}_o + \bar{u}_1 + \bar{c}_1}{2} = \frac{4\bar{c}_o + \gamma - 3}{4} \tag{30}$$

A 5 7 4

Trajectory ob is (integrating eq. (30))

$$\bar{y} = \left(\frac{4\bar{c}_o + \gamma - 3}{4}\right)\bar{t} \tag{31}$$

and of course the trajectory of the payload ab is

$$\bar{y} = 1 - \bar{t} \tag{32}$$

From equations (31) and (32), solve for $\bar{y} = \bar{y}_b$ and $\bar{t} = \bar{t}_b$

$$\bar{y}_b = \frac{4\bar{c}_o + \gamma - 3}{4\bar{c}_o + \gamma + 1} \tag{33}$$

$$\bar{t}_b = \frac{4}{4\bar{c}_o + \gamma + 1} \tag{34}$$

It is possible to stop at this point and compute $\bar{p}_2$ which would give all the information needed to start the integration of equations (20) and (13). However, we also want to have some understanding of the extent of the simple wave region so that we know whether or not the shock cd reflects off the payload before the payload comes to rest. If that were the case, we would be out of the simple wave region, and the simple model would be invalid for that part of the motion after the reflection at d. An approximate knowledge of the location of point d will satisfy present purposes; so in the interest of simplicity, straight lines will be used for both bc and cd. The computation of the pressure and motion

in the simple wave along bd is not affected. Only the location of d is affected.[2] The straight line bc is determined by integrating the equation

$$\left(\frac{d\bar{y}}{d\bar{t}}\right)_{12} \equiv \frac{\bar{u}_1 - \bar{c}_1 + \bar{u}_2 - \bar{c}_2}{2} = -\frac{4\bar{c}_o + 3\gamma - 1}{4} \tag{35}$$

which leads to

$$\bar{y} = -\left(\frac{2\bar{c}_o + 3\gamma - 1}{4}\right)\bar{t} + 4\left(\frac{2\bar{c}_o + \gamma - 1}{4\bar{c}_o + \gamma + 1}\right) \tag{36}$$

When $\bar{y} = 0$, $\bar{t} = \bar{t}_c$

$$\bar{t}_c = \frac{16(2\bar{c}_o + \gamma - 1)}{(4\bar{c}_o + \gamma + 1)(4\bar{c}_o + 3\gamma - 1)}$$

State 3 at the ground is given by

$$\bar{c}_3 = \bar{c}_2 + \frac{\gamma - 1}{2}(\bar{u}_3 - \bar{u}_2) = \bar{c}_o + \frac{3}{2}(\gamma - 1) \tag{37}$$

The slope at the ground of the reflected shock cd is

$$\left(\frac{d\bar{y}}{d\bar{t}}\right)_{23} = \frac{\bar{u}_2 + \bar{c}_2 + \bar{u}_3 + \bar{c}_3}{2} = \frac{4\bar{c}_o + 5\gamma - 7}{4} \tag{38}$$

The equation of the straight line cd is (integrating (38) and saying $\bar{y}_c = 0$ at $\bar{t} = \bar{t}_c$)

$$\bar{t} = \frac{4}{4\bar{c}_o + 5\gamma - 7}\bar{y} + \frac{16(2\bar{c}_o + \gamma - 1)}{(4\bar{c}_o + \gamma + 1)(4\bar{c}_o + 3\gamma - 1)} \tag{39}$$

---

[2]It can be shown that bc curves right, but that cd may curve left or right. If both bc and cd curve right, the straight lines give a conservative location for d inasmuch as solutions will be obtained for which the payload comes nearly to rest before the approximate d is reached in advance of the exact d. Also, if bc curves right and cd curves left, one counteracts the other, and the straight line is probably satisfactory.

The intersection of (39) with the payload trajectory obtained by the simultaneous integration of equations (20) and (13) gives point d.

Next $\bar{p}_2$ is evaluated by the series expansion (ref. 12, p. 1011)

$$\frac{\bar{p}_1}{\bar{p}_0} \equiv 1 + \frac{\gamma(\bar{u}_1 - \bar{u}_0)}{\bar{c}_0} + \frac{\gamma(\gamma + 1)}{4}\left(\frac{\bar{u}_1 - \bar{u}_0}{\bar{c}_0}\right)^2 + \ldots \qquad (40)$$

or

$$\frac{\bar{p}_1}{\bar{p}_0} = \frac{4\bar{c}_0^2 + 4\bar{c}_0\gamma + \gamma^2 + \gamma}{4\bar{c}_0^2} \qquad (41)$$

$$\frac{\bar{p}_2}{\bar{p}_1} = 1 - \gamma\left(\frac{\bar{u}_2 - \bar{u}_1}{\bar{c}_1}\right) + \frac{\gamma(\gamma + 1)}{4}\left(\frac{\bar{u}_2 - \bar{u}_1}{\bar{c}_1}\right)^2 + \ldots \qquad (42)$$

or

$$\frac{\bar{p}_2}{\bar{p}_1} = \frac{4\bar{c}_0^2 + 4(2\gamma - 1)\bar{c}_0 + 4\gamma^2 - 3\gamma + 1}{4\bar{c}_0^2 + 4(\gamma - 1)\bar{c}_0 + (\gamma - 1)^2} \qquad (43)$$

From (41) and (43) since $\bar{p}_0 = 1$

$$\bar{p}_2 = \frac{[4\bar{c}_0^2 + 4(2\gamma - 1)\bar{c}_0 + 4\gamma^2 - 3\gamma + 1][4\bar{c}_0^2 + 4\gamma\bar{c}_0 + \gamma(\gamma + 1)]}{4\bar{c}_0^2[4\bar{c}_0^2 + 4(\gamma - 1)\bar{c}_0 + (\gamma - 1)^2]} \qquad (44)$$

Thus the problem is completely formulated by the series expansion method. To solve a given case, one specifies $\bar{c}_0$, γ, K, m_b/m_p, and $\bar{p}_a$. Then equations (20) and (13) are integrated simultaneously subject to boundary conditions (21), (33), and (34) where $\bar{c}_2$ and $\bar{p}_2$ are calculated from equations (29) and (44). Each example should be checked to be sure that $\bar{u} = 0$ by the time the intersection d has been reached (by use of eq. (39)).

Exact shock relations.- If $\bar{c}_0 < 1$, it was stated (for $\gamma = 1.41$) the exact shock relations or the strong shock approximation must be used for the computation of $\bar{p}_2$ to be accurate. It was also mentioned that for impact without an atmosphere, $\bar{p}_2$ must be 10 or more for the wave model to be valid. This requires that $\bar{c}_0$ be less than 1 and thus the exact shock relations need be used to determine the starting conditions ($\bar{c}_2$, $\bar{p}_2$, $\bar{y}_b$, $\bar{t}_b$) for integration of the differential equations (20) and (13). In addition, the assumed straight line trajectories, bc and cd, should be computed by the exact shock equations.

In sketch (e), the shock represented by the solid line is moving into the gas at state i with speed $\pm\bar{W}_{ij}$ relative to the gas at state i. The gas on the backside of the shock is at state j. The plus sign on $\bar{W}_{ij}$ denotes upward traveling shocks (with respect to gas at state i) and the minus sign denotes downward traveling shock waves. The subscripts i and j used to denote states i and j will eventually take on the pairs of values 01, 12, 23 when the shock relations are applied to the shocks connecting states 0 and 1, 1 and 2, and 2 and 3 in sketch (d). The exact shock relations made dimensionless by equations (8) and (14) are (see ref. 12, pp. 1001, 1002)

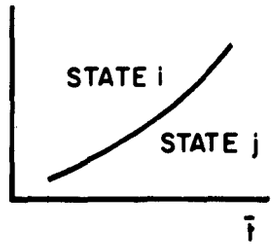

Sketch (e)

$$\left(\frac{d\bar{y}}{d\bar{t}}\right)_{\text{shock ij}} = \bar{u}_i \pm \bar{W}_{ij} = \frac{1}{\gamma - 1}\frac{\bar{c}_i^2 - \bar{c}_j^2}{\bar{u}_i - \bar{u}_j} + \frac{\bar{u}_i + \bar{u}_j}{2} \tag{45}$$

$$\frac{\bar{p}_j}{\bar{p}_i} = 1 + \left(\frac{2\gamma}{\gamma + 1}\right)\left[\left(\frac{\bar{W}_{ij}}{\bar{c}_i}\right)^2 - 1\right] \tag{46}$$

$$\left(\frac{\bar{c}_j}{\bar{c}_i}\right)^2 = 1 + \frac{2(\gamma - 1)}{(\gamma + 1)^2}\left[\gamma\left(\frac{\bar{W}_{ij}}{\bar{c}_i}\right)^2 - \left(\frac{\bar{c}_i}{\bar{W}_{ij}}\right)^2 - (\gamma - 1)\right] \tag{47}$$

Solving equation (45) for $\bar{W}_{ij}/\bar{c}_i$ and combining the results with equation (47) yields

$$x_i^4 + A_3 x_i^3 + A_2 x_i^2 + A_1 x_i + A_0 = 0 \tag{48}$$

where

$$x_i = \frac{\bar{W}_{ij}}{\bar{c}_i} \tag{49}$$

and

$$\left.\begin{aligned} A_0 &= -\frac{1}{\gamma} \\ A_1 &= 0 \\ A_2 &= \left[\frac{(\gamma + 1)^2}{4\gamma\bar{c}_i^2} - \frac{\gamma - 1}{\gamma}\right] \\ A_3 &= -\frac{(\gamma + 1)^2}{2\gamma\bar{c}_i} \end{aligned}\right\} \tag{50}$$

The application of the equations to the shocks connecting the ij states 01, is as follows. It is noted that $\bar{u}_0 = -1$, and $\bar{u}_1 = 0$. Equation (48) is solved for x_0 by use of equation (50) where $\bar{c}_1$ is the specified $\bar{c}_0$. The proper root x_0 is selected judiciously by taking that root for which equation (45) is in closest agreement with the approximation equation (30). The pressure $\bar{p}_1$ is calculated by use of x_0 in equations (46) and (49), and $\bar{c}_1$ is obtained from equation (47). Then equation (45) is integrated to give the equation of the line ob (sketch (d)). The intersection of that line with that of equation (32) locates point b.

In a similar manner, equations (45) through (50) are applied successively to the ij states 12 and 23 to give values for $\bar{p}_2$ and $\bar{c}_2$, locate point c, and give an expression for the line cd. The intersection of that line and the trajectory of the payload (resulting from the integration of eqs. (20) and (13)) gives point d on sketch (d).

Thus the information needed to initiate the integration of the equations of motion and that needed to estimate the regime of validity of the simple wave model has been formulated by both a series approximation and the exact shock relations. Finally, it is instructive to consider briefly the simplification that arises when the strong shock approximation is made.

The strong shock approximation.- If the value of $\bar{c}_1$ is small enough, the quantity $(\bar{c}_1/\bar{W}_{ij})$ is small and (ref. 12, p. 1002) the following relationships are valid

$$\pm \frac{\bar{W}_{ij}}{\bar{c}_i} = \frac{\gamma + 1}{2} \frac{\bar{u}_j - \bar{u}_i}{\bar{c}_i} \tag{51}$$

$$\left(\frac{\bar{c}_j}{\bar{c}_i}\right)^2 = \frac{\gamma(\gamma - 1)}{2} \left(\frac{\bar{u}_j - \bar{u}_i}{\bar{c}_i}\right)^2 \tag{52}$$

$$\frac{\bar{p}_j}{\bar{p}_i} = \frac{\gamma(\gamma + 1)}{2} \left(\frac{\bar{u}_j - \bar{u}_i}{\bar{c}_i}\right)^2 \tag{53}$$

and as before

$$\left(\frac{d\bar{y}}{d\bar{t}}\right)_{\text{shock } ij} = \bar{u}_i \pm \bar{W}_{ij} \tag{54}$$

The application of these relationships to obtain the approximate location of points b, c, and d in sketch (d) proceeds the same way as for the exact shock relations except that now it is not necessary to solve the fourth degree equation for $\bar{W}_{ij}/\bar{c}_i$ which can be computed directly from equation (51). For example, point b is obtained by integrating equation (54) using equation (51) and combining the result with equation (32) which yields the simple expression

$$\left.\begin{aligned} \bar{y}_b &= \frac{\gamma - 1}{\gamma + 1} \\ \bar{t}_b &= \frac{2}{\gamma + 1} \end{aligned}\right\} \tag{55}$$

Similarly, the expressions for $\bar{p}_2$ and $\bar{c}_2$ are derived very simply from equations (53) and (52) to be

$$\left.\begin{aligned} \bar{p}_2 &= \frac{\gamma(\gamma + 1)^2}{2\bar{c}_o^{\,2}(\gamma - 1)} \quad \left(\approx \frac{10}{\bar{c}_o^{\,2}} \text{ if } \gamma \text{ is } 1.41\right) \\ \bar{c}_2 &= \frac{\gamma(\gamma - 1)}{2} \end{aligned}\right\} \tag{56}$$

This relationship for $\bar{p}_2$ is quite good if $\bar{c}_o < 1$ and could be used where the series expansion (44) becomes invalid.

Auxiliary Physical Relationships

It is useful to bring other physical considerations to bear on the problem. The problem of the motion of the payload during impact can be solved if γ, $\bar{c}_o$, K, m_b/m_p, and $\bar{p}_a$ are specified. The selection of these quantities, however, may be influenced by consideration of the maximum allowable number of g's acceleration, allowable stress in the bag skin, initial inflating gas temperature, and other conditions. Thus the auxiliary physical quantities should be related to the quantities needed for solving the payload motion.

The maximum acceleration of the payload up to the end of the simple wave regime occurs at state 2 in sketch (d) and is, from equations (12) and (8),

$$\left(\frac{du}{dt}\right)_b = ng_e = \frac{u_o^2}{y_o} K \frac{\bar{p}_2 - \bar{p}_a}{1 + \frac{m_b}{m_p}\bar{y}_b} \tag{57}$$

The circumferential stress in the bag skin is a maximum at state 3 because of p_3. However, the bag need not withstand this pressure as long as failure caused by it does not propagate faster than the shock cd (a nontearing bag material). Then failure at pressures behind cd does not affect the motion of the payload in the simple wave region and the maximum pressure the bag must withstand is p_2. The corresponding circumferential force per unit axial length (for a circular bag) is

$$(N_c)_b = r(p_2 - p_a) = p_o r(\bar{p}_2 - \bar{p}_a) \tag{58}$$

The maximum axial force per unit circumferential length occurs at the top of the bag at state 2 and is (from eq. (4))

$$(N_a)_b = \frac{m_b \bar{y}_b}{2\pi r}\left(\frac{du}{dt}\right)_b \tag{59}$$

where $(du/dt)_b$ is given in equation (57). Combining (58), (59), and (7) yields

$$m_p\left(\frac{du}{dt}\right)_b = \pi r(N_c - 2N_a)_b \tag{60}$$

which shows that N_c will be more than double N_a for a positive acceleration at b. Therefore, the maximum allowable stress is given by equation (58)

$$N_{max} = p_o r(\bar{p}_2 - \bar{p}_a) \tag{61}$$

Application of equation (57) at state 2 using equations (11) and (61) yields

$$1 + \frac{m_b}{m_p}\bar{y}_b = \frac{\pi r N_{max}}{m_p n g_e} \tag{62}$$

Because

$$m_b = 2\pi r y_o \rho_s \tag{63}$$

(where ρ_s is the mass of skin per unit area), equation (62) becomes

$$\frac{m_b}{m_p} = \frac{1}{\frac{N_{max}/\rho_s}{2y_o n g_e} - \bar{y}_b} \tag{64}$$

Combining equation (64) with equation (57) yields another useful relationship

$$u_o^2 = \frac{(m_b/m_p)(N_{max}/\rho_s)}{2K(\bar{p}_2 - \bar{p}_a)} \tag{65}$$

If the total mass of the system is

$$m = m_g + m_p + m_b + m_{bottom} \tag{66}$$

(where m_{bottom} is the mass of the bag bottom) and the same material is used for the bag sides and bottom so that

$$m_{bottom} = \pi r^2 \rho_s = \frac{m_b r}{2y_o} \tag{67}$$

then

$$\frac{m_p}{m} = \left[1 + \frac{m_g}{m_p} + \frac{m_b}{m_p}\left(1 + \frac{r}{2y_o}\right)\right]^{-1} \tag{68}$$

Briefly, to solve a practical impact problem, one may proceed as follows: Specify γ, $\bar{p}_a$, T_o, and u_o. Then calculate $\bar{c}_o$ from

$$\bar{c}_o = \frac{\sqrt{\gamma R T_o}}{|u_o|} \tag{69}$$

Also calculate $\bar{p}_2$, $\bar{c}_2$ and $\bar{y}_b$ from equations (44), (29), and (33) (if $\bar{c}_o \geq 1$) or by the use of equations (46), (47), and (45) with associated relationships (if $\bar{c}_o < 1$); or use curves which will be presented subsequently to determine $\bar{p}_2$, $\bar{c}_2$, and $\bar{y}_b$. Specify N_{max}/ρ_s. Use equation (65) to obtain a suitable set of values of m_b/m_p and K by trial and error, so that for the $\bar{c}_o$ calculated, m_b/m_p and K fall within the regime of validity of the theory. (Use of a subsequent figure of regimes of validity will be helpful.) This guarantees that N_{max} will not be exceeded. Calculate m_g/m_p from equation (11). Specify r/y_o (with buckling considered as noted earlier). Calculate m_p/m from equation (68). Finally, specify n and calculate y_o from equation (64) and thus r is determined. The motion of the payload is, of course, determined when the necessary quantities are used as inputs to solve equations (20) and (13) simultaneously.

RESULTS

The differential equations (20) and (13) subject to boundary conditions (21) were integrated numerically using the Adams-Moulton (ref. 13, p. 200, eqs. 6.6.2) predictor corrector method on an IBM 704 electronic data processing machine. Initial conditions for the integration were obtained by both the approximate and the exact methods described. These are presented and compared in the first three figures. Results obtained by the actual numerical integration are presented in the last three figures.

Figure 1 is a comparison of the first two methods of computing $\bar{p}_2$. It is seen that for large values of $\bar{c}_0$, either the exact shock relations or the series expansion method (eq. (44)) gives the same value of $\bar{p}_2$. At $\bar{c}_0 = 1$, the series method gives a value of $\bar{p}_2$ approximately 10 percent lower than the exact method. For this reason, the series method should not be used for values of $\bar{c}_0 < 1$. However, for values of $\bar{c}_0 < 1$, the strong shock approximation (eq. (56)) is sufficiently accurate that it cannot be distinguished from the exact shock relations on the figure. Since $\bar{p}_2$ was computed assuming that $\bar{u}_2 = -1$ (i.e., line ab in sketch (d)) is straight), the criteria derived for the validity of the wave model apply to the figure. Thus the regime for $\bar{p}_2 \leq 10$ ($\bar{c}_0 \geq 1$) is not valid if $\bar{p}_a = 0$. For $\bar{p}_2 > 10$ ($\bar{c}_0 < 1$) the wave model is valid for $\bar{p}_a \geq 0$.

In many places in the analysis, the quantity $\bar{y}_b$ appears in physical relationships. Like $\bar{p}_2$, it has been computed by the series expansion equation (33), exact shock relations, and the strong shock approximation equation (55) and is shown in figure 2. The restrictions on the applicability of the curves to the left and right of $\bar{c}_0 = 1$ noted here are the same as those on the $\bar{p}_2$ curves of figure 1. In its range of applicability, the series expansion yields good agreement with the exact shock relations for $\bar{y}_b$, and the two methods yield almost identical results for values of $\bar{c}_0 > 4$. The strong shock approximation, however, gives a value of $\bar{y}_b$ independent of $\bar{c}_0$ as shown.

The quantity $\bar{c}_2$ required for the integration of equation (20) is presented in figure 3. Like $\bar{p}_2$ and $\bar{y}_b$, it has been computed by the exact method, the series expansion equation (29), and the strong shock approximation (56), and has the same limitations imposed above. The series and the exact methods give very good agreement, but the strong shock approximation gives a crude single value of $\bar{c}_2$.

The regime of validity of the simple wave model for $\bar{p}_a = 1$ is shown in figure 4. The lower limit for the series solution is at $\bar{c}_0 = 1$ and corresponds to the limit on use of series shock relations. Thus the series shock relations are valid in most of the regime of validity of the simple wave model. The upper limits on $\bar{c}_0$ (mentioned earlier) for the

various values of m_b/m_p correspond to the situation in which the second shock, cd in sketch (d), just gets to the payload as it comes to rest. It is an approximate limit on the regime of the simple wave model.

A corresponding plot of the regime of validity for the case $\bar{p}_a = 0$ is shown in figure 5. The same comments apply except that part of the upper limit is determined by the value $\bar{c}_o \approx 1$ to insure that $\bar{p}_2 \geq 10$ in accord with the criteria developed in the analysis. Thus, application of the present wave model to impact without atmosphere is limited essentially to situations in which $0 \leq \bar{c}_o \leq 1$.

The solutions of the differential equations (20) and (13) are presented in figure 6 for one impact condition. The solutions were obtained by use of both series and exact methods for a value of $\bar{c}_o = 1.874$ (which is not expected to give outstanding agreement). The differences in $\bar{y}_b$ and $\bar{y}_{min}$ between the two methods are about 2 and 5 percent, respectively. The difference in $\bar{p}_2$ is about 3 percent. The velocity computed by the series method decays at about the same rate as that computed by the exact method but lags by about 5 percent of the initial speed at any given instant. Thus the agreement between the two methods is satisfactory.

CONCLUDING REMARKS

A theory of impact cushioning by use of cylindrical gas bags has been developed. The theory is applicable to high-speed impact conditions because unsteady gas dynamic phenomena have been incorporated in the analysis by the use of a simplified mathematical model for the waves in the gas. The influence of the bag skin forces on the motion of the payload has also been accounted for in the analysis. The shock waves in the gas are treated by exact relationships, the strong shock approximation, and a series expansion. The last two treatments lead to relatively simple useful physical relationships for analyzing the impact motion. The methods are compared, and the regime of validity of each, as well as the regime of validity of the basic wave model, is evaluated. Curves of some physical results are presented which can be used with equations presented for calculation purposes.

Ames Research Center
National Aeronautics and Space Administration
Moffett Field, Calif., Jan. 12, 1962

REFERENCES

1. Matlock, H., Ripperger, E. A., Turnbow, J. W., and Thompson, J. N.: Energy-Absorbing Materials and Systems. Part II. Structural Mechanics Research Laboratory. The University of Texas, Aug. 1957.

2. Matlock, H., and Thompson, J. N.: Preliminary Tests on a Non-Pressurized Air Bag. Part III. Structural Mechanics Research Laboratory. The University of Texas, Oct. 1957.

3. Karnes, C. H., Turnbow, J. W., Ripperger, E. A., and Thompson, J. N.: High-Velocity Impact Cushioning. Part V. Energy-Absorption Characteristics of Paper Honeycomb. Structural Mechanics Research Laboratory. The University of Texas, May 1959.

4. Turnbow, J. W.: Characteristics of Foamed Plastics Under Dynamic Loading. Part VII. Structural Mechanics Research Laboratory. The University of Texas, March 1957.

5. Turnbow, J. W., and Ogletree, W. B.: The Energy-Dissipating Characteristics of Airbags. Structural Mechanics Research Laboratory. The University of Texas, Aug. 1959.

6. McGehee, J. R., and Hathaway, M. E.: Landing Characteristics of a Reentry Capsule With Torus-Shaped Air Bag for Load Alleviation. NASA TN D-628, 1960.

7. Tomcsak, S. L.: Decelerator Bay Study. WADC TR 59-775, June 1960.

8. Hoffman, E. L., Stubbs, S. M., and McGehee, J. R.: Effect of a Load-Alleviating Structure on the Landing Behavior of a Reentry-Capsule Model. NASA TN D-811, 1961.

9. Esgar, Jack B., and Morgan, William C.: Analytical Study of Soft Landings on Gas Filled Bags. NASA TR R-75, 1960.

10. Martin, E. Dale, and Howe, John T.: An Analysis of the Impact Motion of an Inflated Sphere Landing Vehicle. NASA TN D-314, 1960.

11. Howe, John T., and Martin, E. Dale: Gas Dynamics of an Inflated Sphere Striking a Surface. NASA TN D-315, 1960.

12. Shapiro, A. H.: The Dynamics and Thermodynamics of Compressible Fluid Flow. The Ronald Press, 1954.

13. Hildebrand, F. B.: Introduction to Numerical Analysis. McGraw-Hill Book Company, 1956.

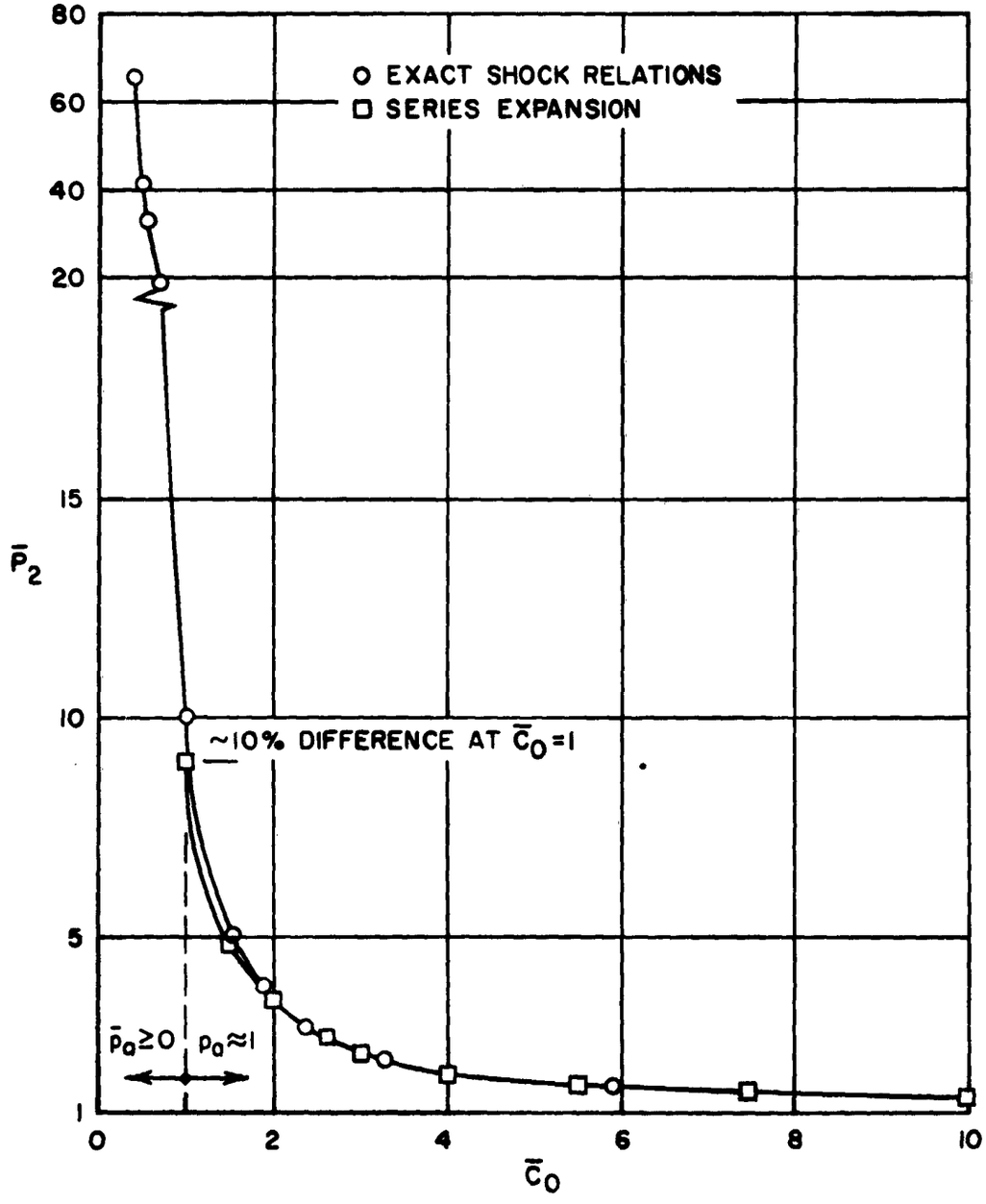

Figure 1.- Curves of $\bar{p}_2$ calculated by both methods; γ = 1.41.

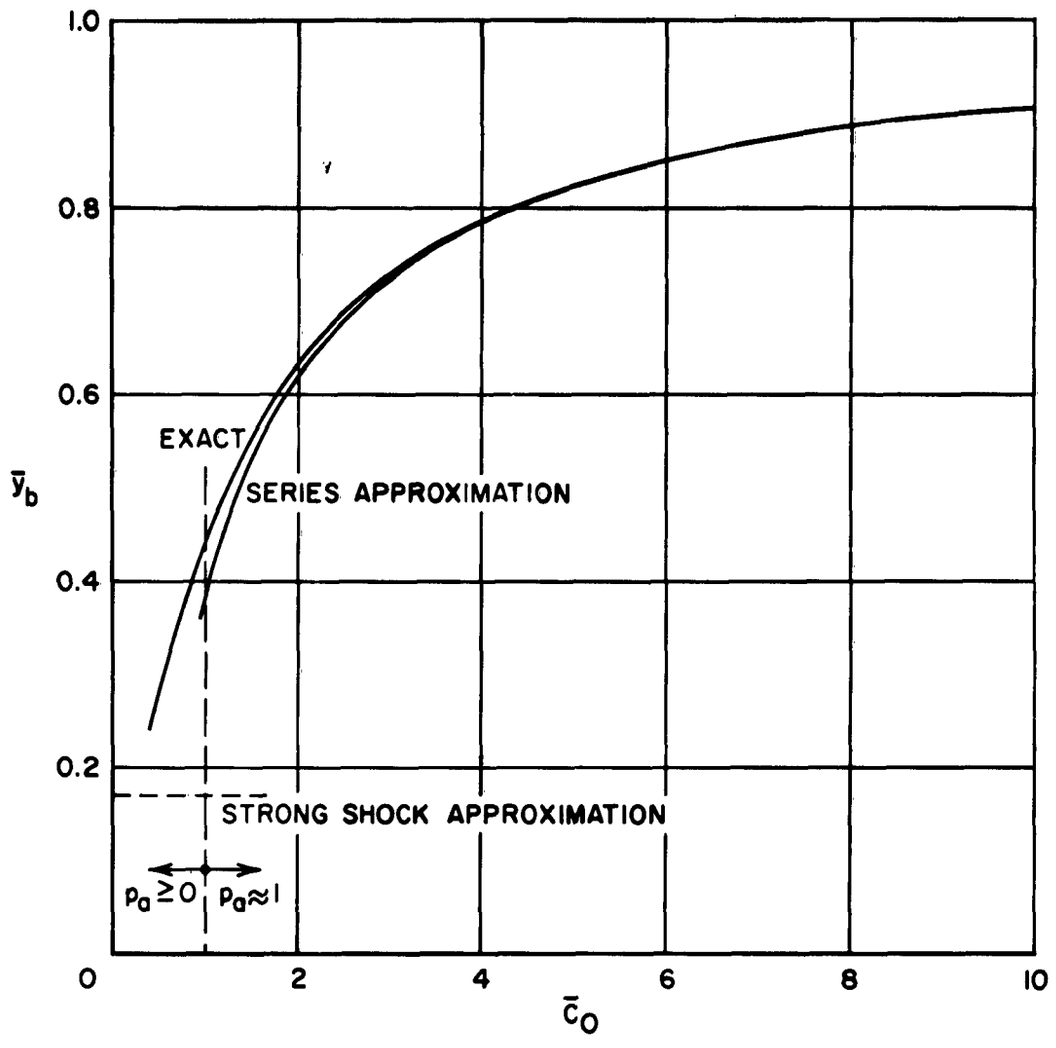

Figure 2.- Height above ground where shock first strikes payload; $\gamma = 1.41$.

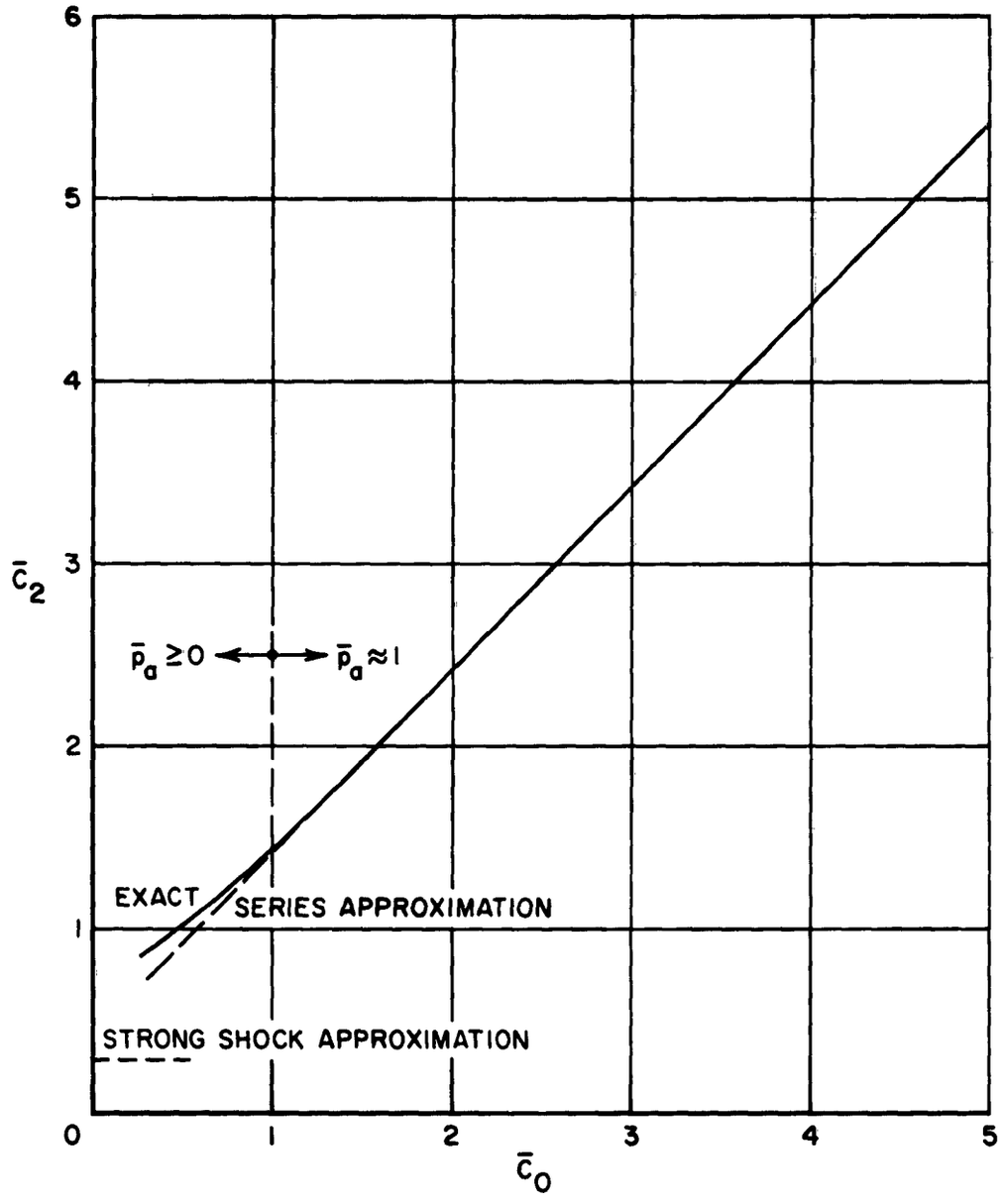

Figure 3.- Sound speed behind the first reflected shock; $\gamma = 1.41$.

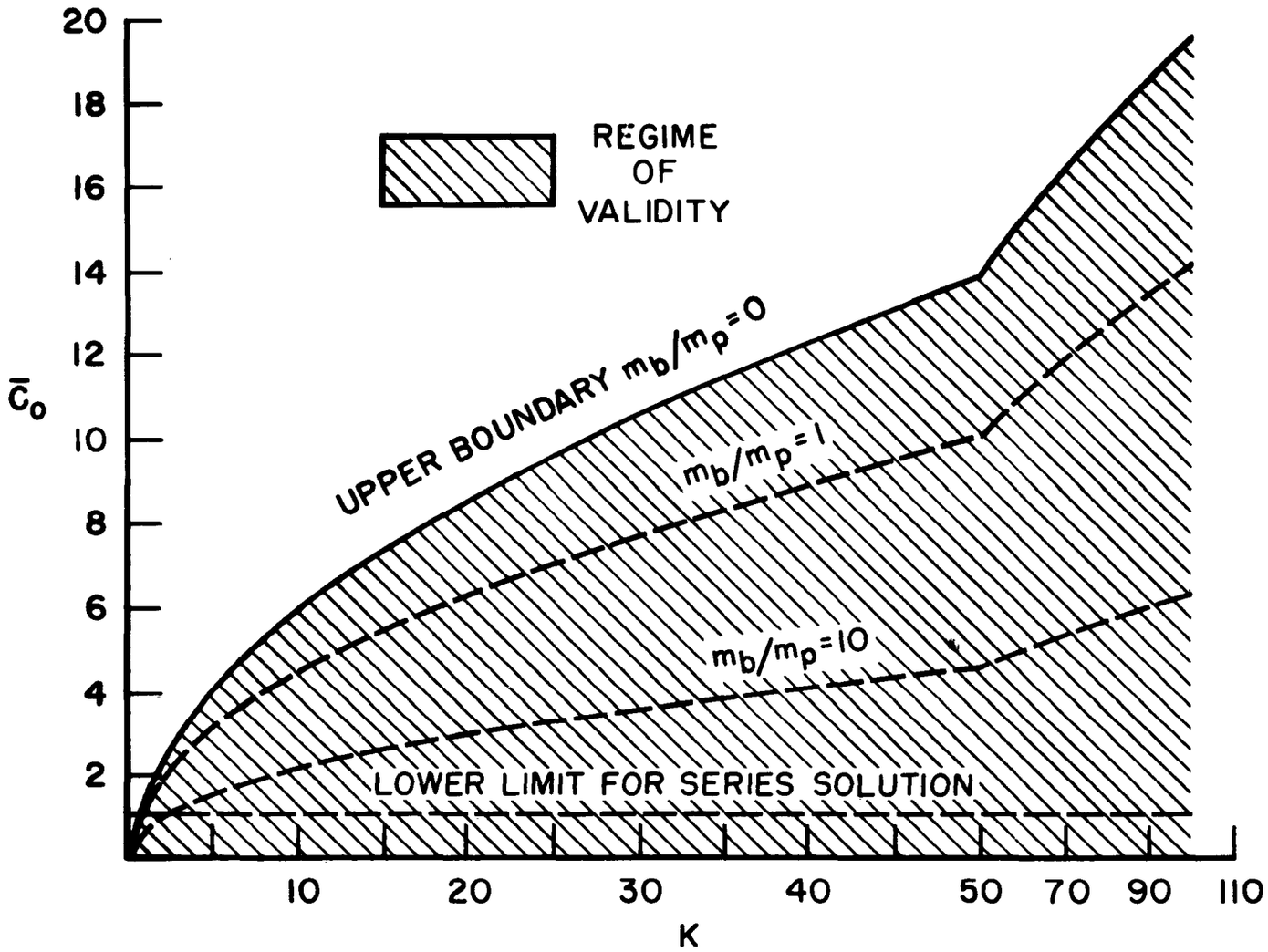

Figure 4.- Regime of validity of simple wave solution; $\bar{p}_a = 1$, $\gamma = 1.41$.

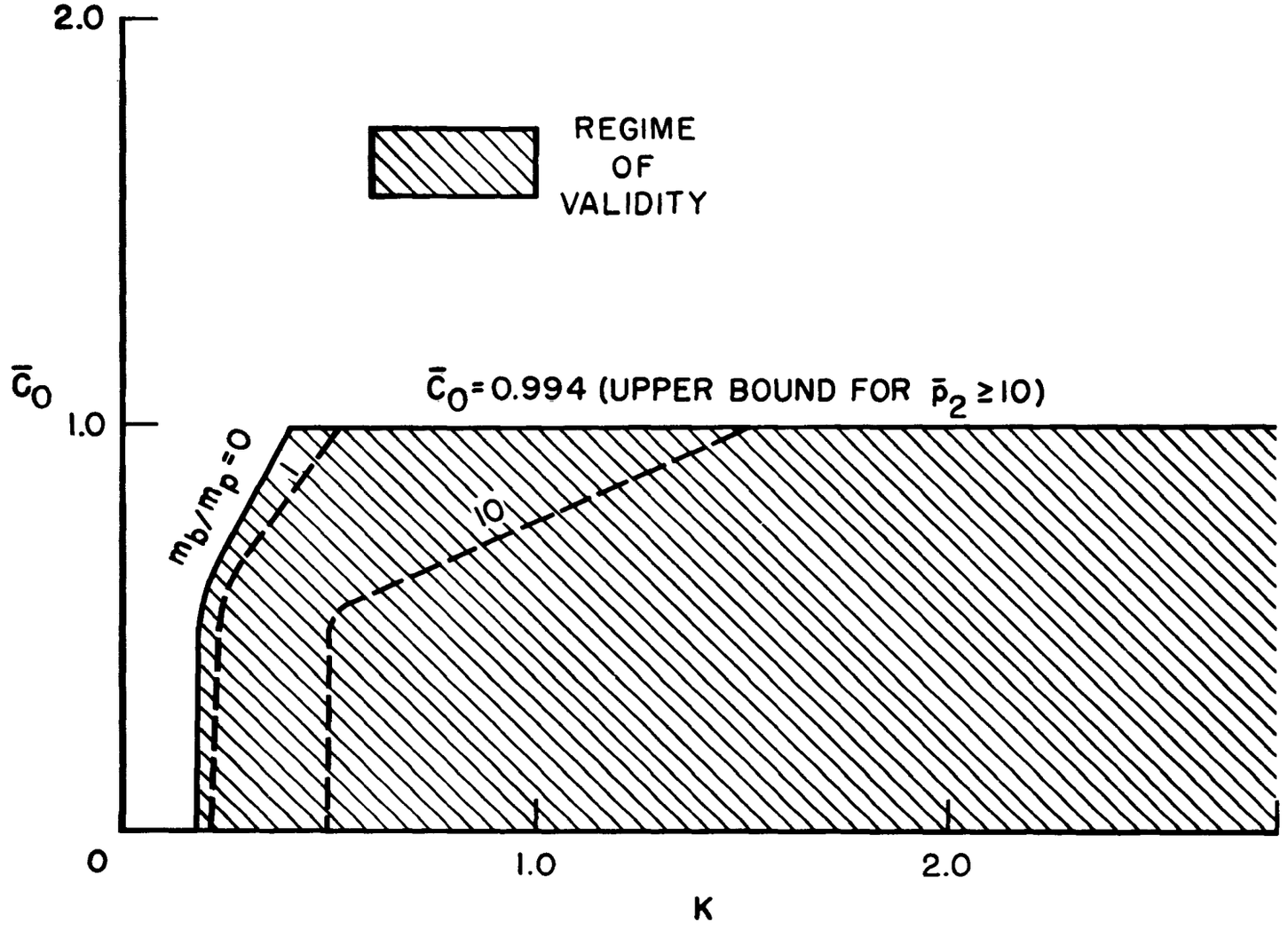

Figure 5.- Regime of validity of simple wave solution; $\bar{p}_a = 0$, $\gamma = 1.41$.

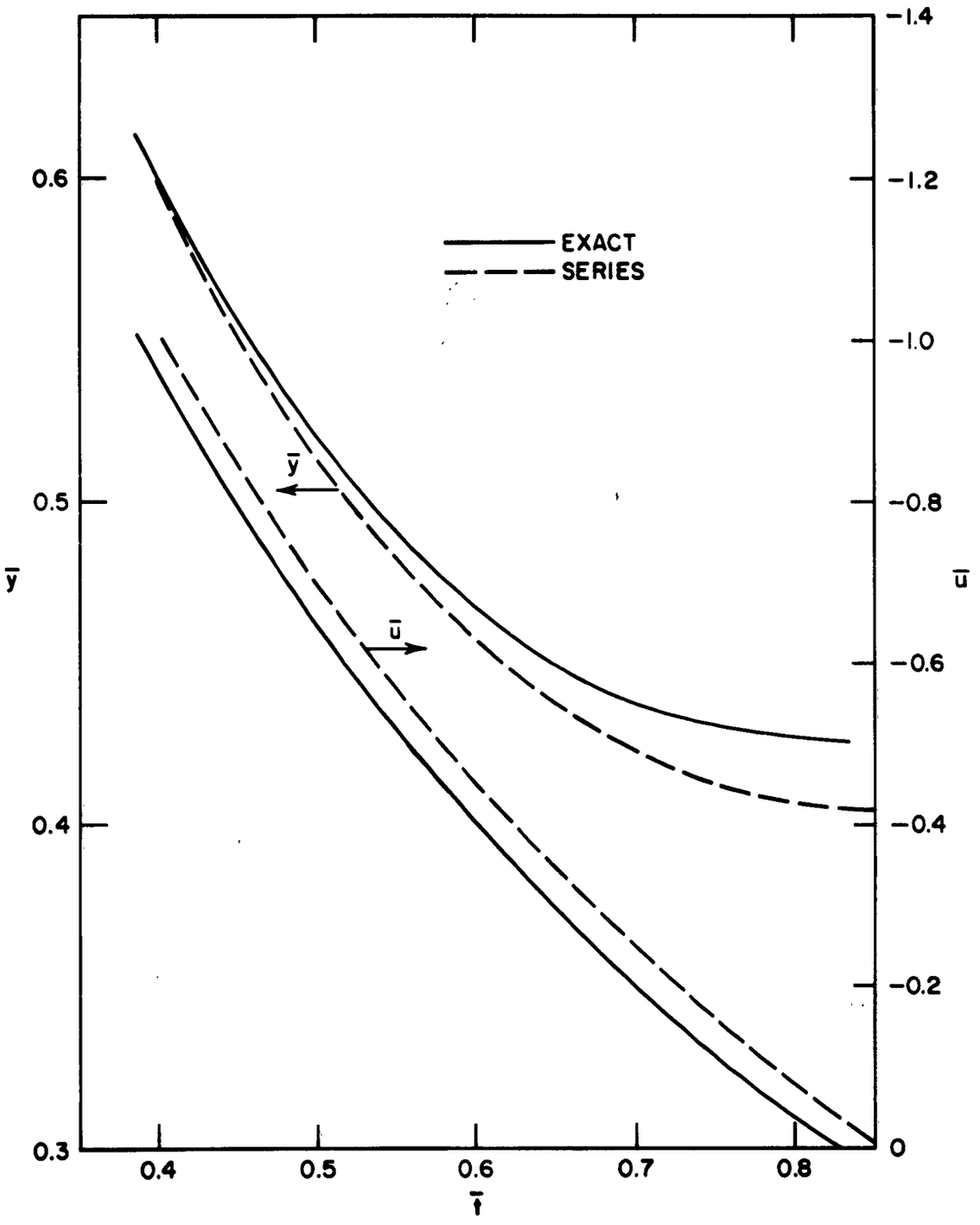

Figure 6.- Comparison between exact and series methods; $\gamma = 1.41$, $\bar{c}_o = 1.874$, $K = 2$, $m_b/m_p = 1$, $\bar{p}_a = 1$.

NASA-Langley, 1962 A-574

NASA TN D-1298
National Aeronautics and Space Administration.
THEORY OF HIGH-SPEED-IMPACT ATTENUATION BY GAS BAGS. John Thomas Howe. April 1962.
28p. OTS price, $0.75.
(NASA TECHNICAL NOTE D-1298)

A theory is developed for the one-dimensional motion of a cylindrical gas bag used as an impact cushion. The effect of shock waves in the gas as well as stress in the bag skin is considered. The applicability of the theory to landings both in an atmosphere and on the moon is discussed and the regime of validity of the theory is presented. The use of a series expansion for computing shock-wave properties in the analysis, the strong shock approximation, and the exact shock relations are compared and discussed. The regime of physical parameters for which both the wave model and the series expansion are valid is presented. The method of application of the theory to impact problems is outlined.

Copies obtainable from NASA, Washington

I. Howe, John Thomas
II. NASA TN D-1298

(Initial NASA distribution:
48, Space vehicles;
51, Stresses and loads.)

NASA

NASA TN D-1298
National Aeronautics and Space Administration.
THEORY OF HIGH-SPEED-IMPACT ATTENUATION BY GAS BAGS. John Thomas Howe. April 1962.
28p. OTS price, $0.75.
(NASA TECHNICAL NOTE D-1298)

A theory is developed for the one-dimensional motion of a cylindrical gas bag used as an impact cushion. The effect of shock waves in the gas as well as stress in the bag skin is considered. The applicability of the theory to landings both in an atmosphere and on the moon is discussed and the regime of validity of the theory is presented. The use of a series expansion for computing shock-wave properties in the analysis, the strong shock approximation, and the exact shock relations are compared and discussed. The regime of physical parameters for which both the wave model and the series expansion are valid is presented. The method of application of the theory to impact problems is outlined.

Copies obtainable from NASA, Washington

I. Howe, John Thomas
II. NASA TN D-1298

(Initial NASA distribution:
48, Space vehicles;
51, Stresses and loads.)

NASA

NASA TN D-1298
National Aeronautics and Space Administration.
THEORY OF HIGH-SPEED-IMPACT ATTENUATION BY GAS BAGS. John Thomas Howe. April 1962.
28p. OTS price, $0.75.
(NASA TECHNICAL NOTE D-1298)

A theory is developed for the one-dimensional motion of a cylindrical gas bag used as an impact cushion. The effect of shock waves in the gas as well as stress in the bag skin is considered. The applicability of the theory to landings both in an atmosphere and on the moon is discussed and the regime of validity of the theory is presented. The use of a series expansion for computing shock-wave properties in the analysis, the strong shock approximation, and the exact shock relations are compared and discussed. The regime of physical parameters for which both the wave model and the series expansion are valid is presented. The method of application of the theory to impact problems is outlined.

Copies obtainable from NASA, Washington

I. Howe, John Thomas
II. NASA TN D-1298

(Initial NASA distribution:
48, Space vehicles;
51, Stresses and loads.)

NASA

NASA TN D-1298
National Aeronautics and Space Administration.
THEORY OF HIGH-SPEED-IMPACT ATTENUATION BY GAS BAGS. John Thomas Howe. April 1962.
28p. OTS price, $0.75.
(NASA TECHNICAL NOTE D-1298)

A theory is developed for the one-dimensional motion of a cylindrical gas bag used as an impact cushion. The effect of shock waves in the gas as well as stress in the bag skin is considered. The applicability of the theory to landings both in an atmosphere and on the moon is discussed and the regime of validity of the theory is presented. The use of a series expansion for computing shock-wave properties in the analysis, the strong shock approximation, and the exact shock relations are compared and discussed. The regime of physical parameters for which both the wave model and the series expansion are valid is presented. The method of application of the theory to impact problems is outlined.

Copies obtainable from NASA, Washington

I. Howe, John Thomas
II. NASA TN D-1298

(Initial NASA distribution:
48, Space vehicles;
51, Stresses and loads.)

NASA